Anal. Bioanal. Electrochem., Vol. 17, No. 9, 2025, 789-802
https://www.doi.org/10.22034/abec.2025.738912

Analytical & Bioanalytical Electrochemistry

Full Paper

Nanocomposite-based Electrochemical Sensor for the Quantification of Totarol in Tetraclinis Articulata Extract

Loubna Kabiri,[1] Omar Anor,[1] Sofia Kerouad,[1] Forsal Issam,[1,*] Mohammed Ellait,[1] and Younes Ziat[2]

[1]*Laboratory of Engineering and Applied Technologies, School of Technology, Beni Mellal, Morocco*
[2]*Engineering and Applied Physics Laboratory (EAPL), Superior School of Technology, Sultan Moulay Slimane University, Beni Mellal, Morocco*

*Corresponding Author, Tel.: +212 661-118208
E-Mail: forsalissam@usms.ma

Received: 22 July 2025 / Received in revised form: 23 December 2025 / Accepted: 24 December 2025 / Published online: 31 December 2025

Abstract- Totarol, a bioactive diterpenoid well known for its potent biological activities, requires precise determination in plant matrices for pharmacological and quality control purposes. However, classical analytical techniques are limited by high costs, complex protocols, and environmental concerns, requiring the development of faster, more sensitive, and greener alternatives. This work presents an innovative carbon paste electrode (CPE) incorporating zinc oxide (ZnO) and magnesium ferrite ($MgFe_2O_4$) nanoparticles was designed to enable the electrochemical quantification of Totarol in Tetraclinis articulata (TA) extract. The electrochemical behavior of Totarol was studied using cyclic voltammetry (CV), electrochemical impedance spectroscopy (EIS), and square wave voltammetry (SWV). The interaction between the both of nanoparticles and Totarol was characterized using scanning electron microscopy (SEM). The ZnO:$MgFe_2O_4$-modified CPE demonstrated remarkable sensitivity towards Totarol, with a low LOD of 1.18 µM and excellent linearity (R^2 = 0.989) over a concentration range of 2.0 to 11.4 mM. The developed sensor enabled the accurate determination of Totarol in the studied plant extract, with a quantified concentration of 0.125 mM. These promising results reveal the potential of the proposed electrode as a simple, efficient, and reliable electrochemical platform for the rapid analysis of bioactive compounds in complex natural matrices.

Keywords- Chemically modified electrodes; Totarol; Nanoparticles, Electrochemical Analysis

1. INTRODUCTION

Throughout history, aromatic and medicinal plants have been essential in multiple fields, particularly due to the presence of bioactive compounds. While extensive research has been done on numerous plant species, there is still limited exploration of forest species, particularly those from the Cupressaceae family [1]. This gap presents an opportunity for an investigation into *Tetraclinis articulata*, a member of the Cupressaceae family. This evergreen tree is resilient to harsh climatic conditions and is indigenous to the Mediterranean region. T. articulata has long been valued in folk medicine for its diverse therapeutic applications [2]. Research has demonstrated that T. articulata extracts exhibit various biological properties, such as antioxidant, insecticidal, antimicrobial, cytotoxic, and anti-inflammatory effects [3,4], highlighting its potential for diverse medicinal applications. One of the key bioactive compounds found in *T. articulata* is Totarol, a phenolic diterpene known for its potent anticancer [5], neuroprotective [6], anti-inflammatory [7] and antimicrobial properties [8,9]. Totarol holds promise for diverse practical uses in medicine [10], cosmetics [11], environmental [12] and food sciences [13,14]. Its chemical structure, rich in hydroxyl groups, facilitates its ability to scavenge free radicals and inhibit the growth of harmful microorganisms. These qualities make Totarol an attractive alternative to synthetic compounds, particularly in the face of growing concerns over the safety and environmental impact of conventional chemical agents.

The growing interest in sustainable and environmentally responsible products has stimulated the exploration of bioactive compounds obtained from natural resources. Among these compounds, Totarol has attracted considerable attention owing to its potential applications in pharmaceutical, cosmetic, and food-related fields. Reliable determination of Totarol content is crucial for ensuring product consistency, maintaining quality standards, and guaranteeing the effectiveness and safety of formulations containing this molecule. Accurate analytical methods are therefore required to monitor its concentration in plant extracts and commercial products.

Electrochemical methods stand out as particularly well-suited analytical tools for this purpose, owing to their inherent sensitivity, rapid response, and compatibility with complex sample matrices. In this work, a CPE modified with a ZnO–$MgFe_2O_4$ nanocomposite was developed and applied for the electrochemical detection of Totarol, taking advantage of the nanocomposite's synergistic properties, namely its extended active surface area, enhanced electron transfer kinetics, and electrocatalytic activity toward phenolic compounds [15,16]. The electroanalytical behaviour of the electrode was studied using CV to elucidate the redox mechanism of Totarol, EIS to characterize the interfacial charge transfer properties of the modified electrode, and SWV for sensitive and quantitative determination of Totarol in Tetraclinis articulata extract. The integration of the ZnO:$MgFe_2O_4$ as a modifier proved

instrumental in achieving a low LOD, positioning the developed sensor as a reliable platform for Totarol monitoring in real matrices.

To date, there have been no reports utilizing modified electrodes for the electrochemical detection of Totarol, which positions this research as a pioneering effort in the field. This approach not only offers a more efficient alternative to traditional methods of Totarol analysis, but also demonstrates the potential of modified electrodes to enhance the specificity and sensitivity of detection. The ability to quantify Totarol using electrochemical sensors opens up new avenues for the rapid, in situ analysis of bioactive compounds in natural products, which could have significant implications for pharmaceutical, environmental, and quality control applications. By addressing a gap in current research, this study paves the way for further advancements in the electrochemical sensing of plant-derived bioactive compounds.

2. EXPERIMENTAL SECTION

2.1. Reagents

All reagents are of analytical purity and were utilized without purification. Sodium hydroxide (NaOH), sodium chloride (NaCl), zinc chloride ($ZnCl_2$), and graphite powder were purchased from Sigma-Aldrich.

2.2. Equipment

Electrochemical performance was carried out using an OrigaStat 100 potentiostat/galvanostat controlled by OrigaMaster 5 software. A 3-electrode cell configuration was utilized throughout the experiments, consisting of the ZnO–$MgFe_2O_4$/CPE as the working electrode, a platinum wire as the counter electrode, and a saturated calomel electrode (SCE) as the reference electrode. Morphological analysis was conducted using a scanning electron microscope (SEM) fitted with FEG 450. FT-IR spectra of the synthesized ZnO were recorded on a JASCO FT/IR-4600 spectrometer operating in attenuated total reflectance (ATR) mode. Spectra were collected over the wavenumber range of 600–4000 cm^{-1} at a spectral resolution of 4 cm^{-1}, with 16 scans accumulated per measurement.

2.3. Synthesis of ZnO NPs

ZnO Nps were prepared via a co-precipitation using $ZnCl_2$ and NaOH as precursor materials. The stoichiometric relationship governing the reaction is described by the following equation:

$$ZnCl_2 + 2NaOH \longrightarrow Zn(OH)_2 + 2NaCl \quad (1)$$

A 1 M NaOH solution was introduced dropwise into a 0.5 M solution of $ZnCl_2$ under continuous stirring. The mixture was maintained under constant stirring for 2 h, after which the

suspension was sealed and allowed to age overnight. The obtained precipitate was then filtered, washed, and dried at 100 °C for 12 h. The powder was then calcined at 300 °C for 4 h [17].

2.4. Synthesis of $MgFe_2O_4$ NPs

The synthesis method and characterization of $MgFe_2O_4$ NPs were described by Sofia et al [18].

2.5. Preparation of the sensor

The ZnO–$MgFe_2O_4$/CPE was fabricated by manually homogenizing 0.05 g of ZnO, 0.05 g of $MgFe_2O_4$, and 0.85 g of graphite. The dry mixture was blended with 0.5 mL of paraffin oil and blended for 0.5 h until obtained a homogeneous paste of uniform consistency. The mixture was then packed into a syringe tube, and electrical contact was established by inserting a copper wire through the tube. The CPE was prepared with the same procedure without adding nanoparticles [19].

2.6. Preparation of Tetraclinis articulata

A continuous extraction of 500g of sawdust of *T. articulata* by dichloromethane in a Soxhlet apparatus was performed. After 24 hours of extraction, 45.6 g (9.2% yield) of the pungent brown-black dichloromethane residue was obtained. This extract was then preserved for the subsequent quantification of Totarol content [20].

3. RESULTS AND DISCUSSION

3.1. Characterization of ZnO

The FT-IR spectra of ZnO is presented in Fig. 1. The absorption band observed at 400 cm^{-1} is assigned to the Zn–O stretching vibration, confirming the formation of the ZnO phase [21].

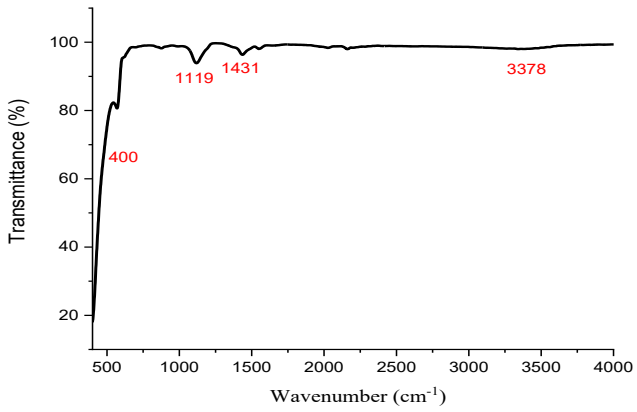

Figure 1. FTIR spectra of ZnO NPs

The broad band centered at 3378 cm^{-1} and the peak at 1431 cm^{-1} are attributed to the O–H vibration arising from adsorbed water molecules [22]. Additionally, the band appearing at 1119 cm^{-1} is ascribed to C–O stretching vibrations [23].

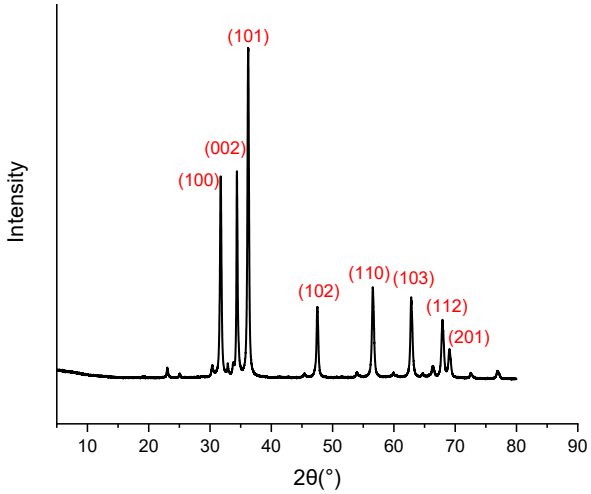

Figure 2. XRD pattern of ZnO NPs

The XRD pattern of ZnO NPs shown in Fig. 2, reveals a series of peaks at 31.0°, 34.4°, 36.1°, 47.0°, 56.0°, 63.0°, 68.0°, and 69.0°, indexed to the (100), (002), (101), (102), (110), (103), (112), and (201) crystallographic planes [24]. These data indicate the successful formation of ZnO NPs and are consistent with previous literature reports [25,26].

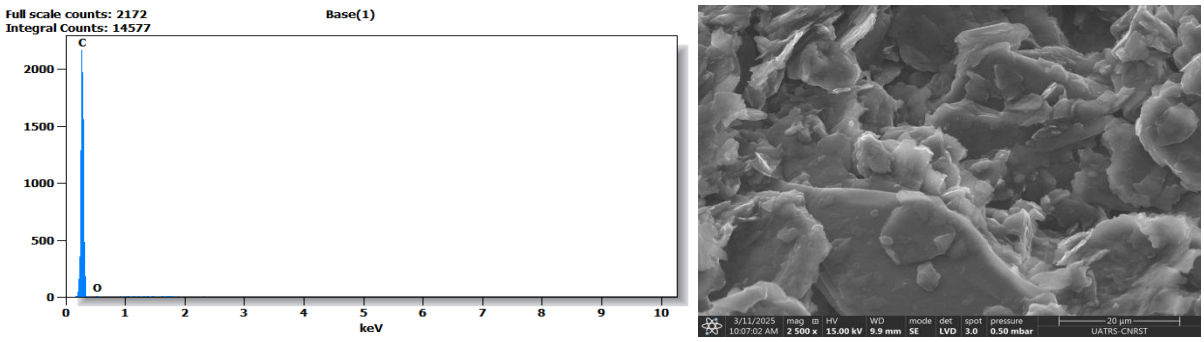

Figure 3. SEM and EDX of CPE

The analysis of the modified electrode surface, conducted after 20 min of preconcentration in a 2 mM Totarol (Figure 5), reveals the presence of small clusters that correspond to the accumulation of Totarol molecules onto the nanocomposite surface. Notably, these clusters are remarkable relative to those observed on the electrode surface prior to Totarol exposure (Figure

4). These findings confirm the successful surface modification of the CPE with the ZnO–$MgFe_2O_4$ nanocomposite and its capacity to retain Totarol at the electrode interface [27].

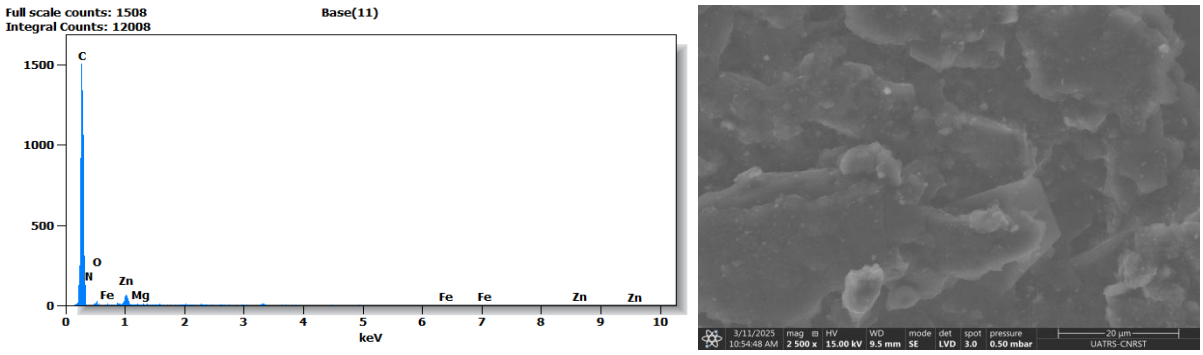

Figure 4. SEM and EDX of ZnO:$MgFe_2O_4$/CPE

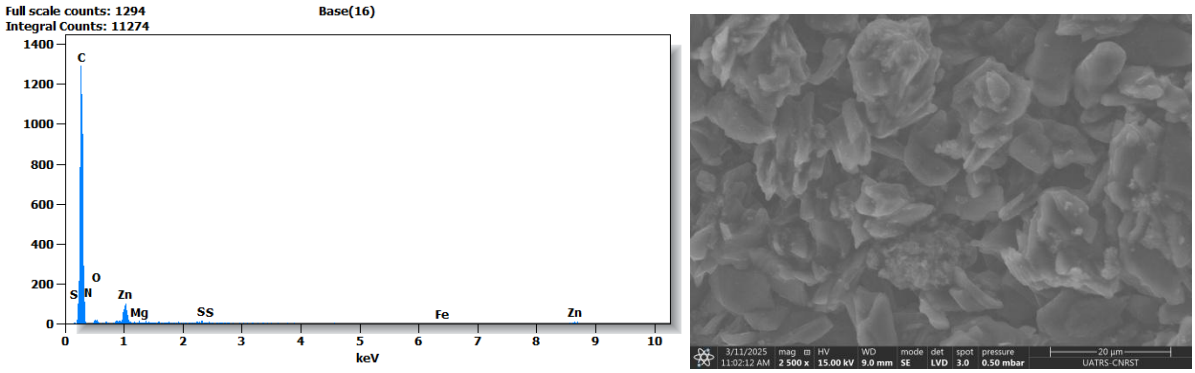

Figure 5. SEM and EDX of ZnO:$MgFe_2O_4$/CPE after 20 min in 2mM of Totarol

3.2. Electrochemical attitude of Totarol on the sensors

3.2.1. CV

The performance of Totarol at the ZnO–$MgFe_2O_4$/CPE and CPE was examined by CV in 0.1 M NaCl. Fig. 6 illustrated the C. voltammograms for both electrodes in the presence of 2 mM Totarol at a SR of 80 mV/s over a potential window of −2.0 to +1.0 V. It is evident that no current signal is observed for the oxidation/reduction of Totarol at the CPE; In contrast, an oxidation peak was present at the ZnO–$MgFe_2O_4$/CPE with a peak current of 1.80 mA, reflecting a significant enhancement in electrochemical reactivity. This enhancement is due to the high density of electroactive sites provided by the nanocomposite, which facilitates greater analyte accessibility to the electrode surface and promotes Totarol adsorption through the extended surface area of the ZnO–$MgFe_2O_4$ [28]. These results demonstrate that the sensor is suitable for the determination of Totarol.

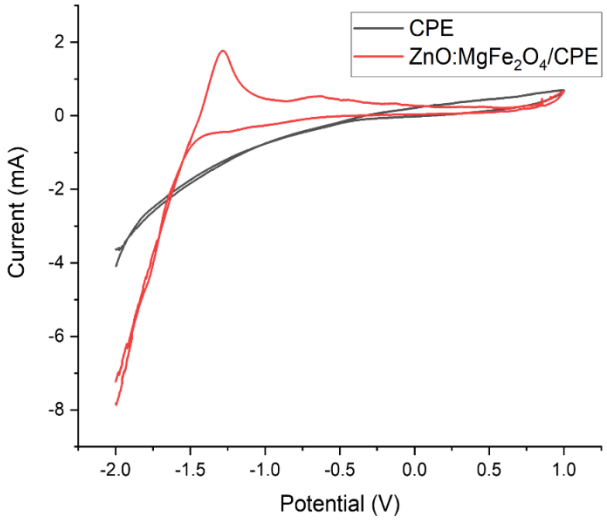

Figure 6. CV of sensors with 2 mM of Totarol in 0.1 M NaCl (pH 4.5) at a SR of 80 mV/s. RE: Hg/Hg_2Cl_2, KCl_{sat}

3.2.2. EIS

EIS was applied to study the interfacial characteristics of the electrodes across a frequency range of 100 mHz to 1 kHz. Figure 7 illustrates the Nyquist plots for the electrodes exposed to 2 mM Totarol. The semicircle diameter observed for the ZnO–$MgFe_2O_4$/CPE is markedly reduced relative to that of the CPE, indicating a lower charge transfer resistance Rct and confirming that the incorporation of the nanocomposite considerably enhances the interfacial charge transport ability at the sensor surface. Furthermore, the appearance of a Warburg impedance suggests that the mechanism governing Totarol oxidation is predominantly controlled by mass transport [29].

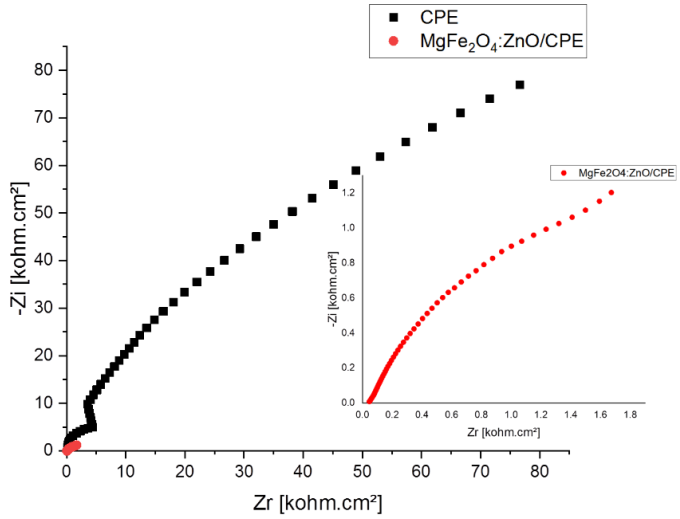

Figure 7. Nyquist plots of sensors with 2 mM of Totarol in a 0.1 M NaCl; pH=4.5; FR:100kHz–10 mHz. RE: Hg/Hg_2Cl_2, KCl_{sat}

3.3. Parameter optimization

3.3.1. SR effect

The logarithmic plot of peak current vs SR (Fig. 8B) yields a slope of 0.451, consistent with the theoretical value of 0.5 expected for a diffusion mechanism, indicating that mass transport governs the reaction of Totarol at the modified sensor. This conclusion is further corroborated by the linear relationship between Ipa and $v^{1/2}$ depicted in Fig. 8C, which affords a $R^2 = 0.97$, consistent with Fick's law of diffusion [30]. These observations indicate that the oxidation of Totarol at the ZnO: $MgFe_2O_4$/CPE is influenced by diffusion [31].

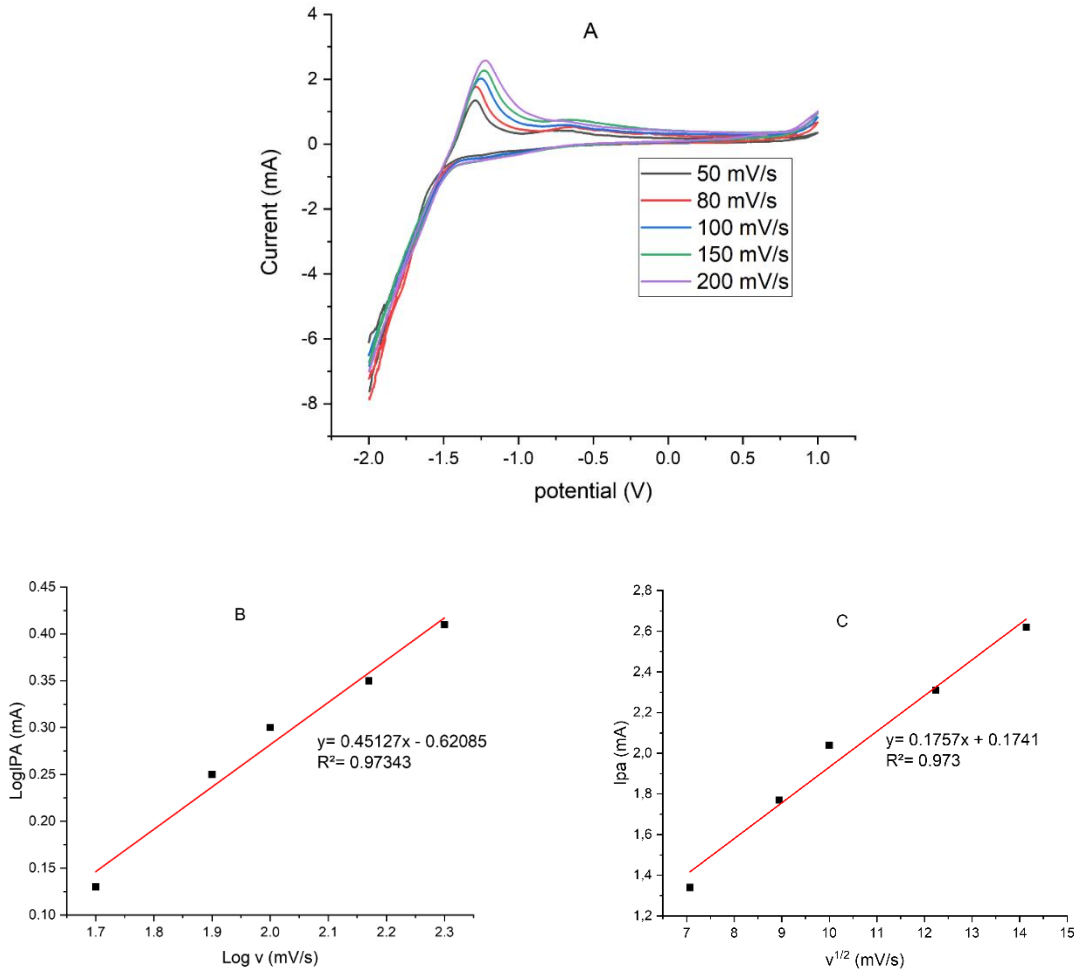

Figure 8. (A) CV of the sensor in 0.1 M NaCl (pH= 4.5) with 2 mM of Totarol at various SRs. RE: Hg/Hg_2Cl_2, KCl_{sat} (B) Plot of log I_{pa} *vs* log of SR. (C) Plot of I_{pa} *vs* $v^{1/2}$

3.3.2. pH effect

The pH range of 2.5 to 8.5 was used to examine the impact of the solution on the electrode behavior. As illustrated in Figure 9A; the top current peak is seen at pH 5.5, indicating that this is the optimum pH for the identification of Totarol.

To gain insight into the number of protons and electrons included in the oxidation of Totarol, the relationship between Epa and solution pH was examined using Eq. (2) [32]:

$$Ep= -2.303\ (m/n)\ (RT/F) \qquad (2)$$

where m/n represents the proton-to-electron transfer ratio. As depicted in Fig. 9B, the linear plot of E_{pa} versus pH yields a slope of 30.7 mV/pH, which is in close agreement with the theoretical Nernstian value of 29.5 mV/pH, characteristic of a 2-electron, 1-proton transfer mechanism [33,34]. On this basis, a plausible mechanistic pathway is proposed:

$$\text{Totarol-(OH) (adsorbed on ZnO:MgFe}_2\text{O}_4) \longrightarrow \text{Totarol}^{-}(\text{O}^{ox}) + \text{H}^{+} + 2\text{e}^{-} \qquad (3)$$

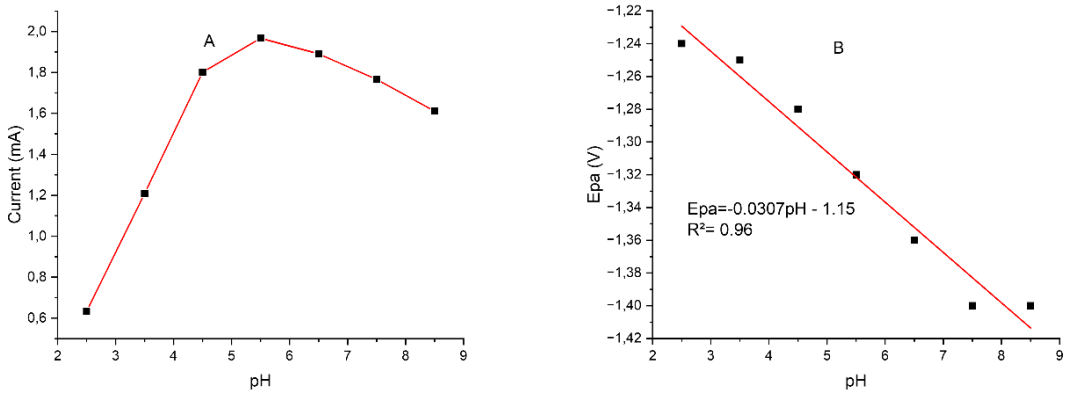

Figure 9. (A) Effect of pH on peak current of Totarol in 0.1 M NaCl at a SR of 80 mV/s. RE: Hg/Hg_2Cl_2, KCl_{sat} (B) Plot of E_{pa} *vs.* pH

3.3.3. Preconcentration effect

The influence of the preconcentration for the detection of the Totarol was investigated between 0 to 7min in 0.1 M NaCl at pH=5.5 containing 2 mM of Totarol.

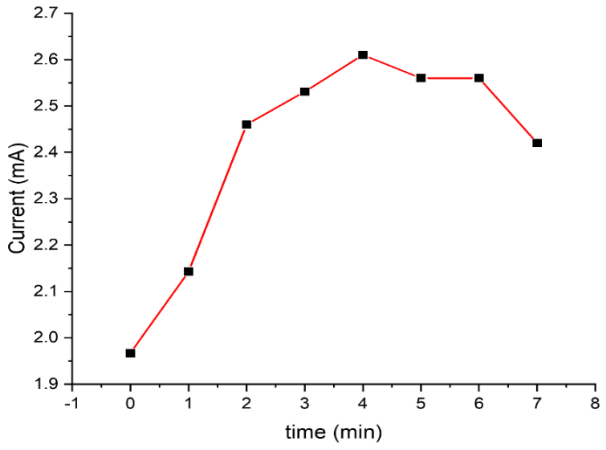

Figure 10. Effect of preconcentration on the peak current of the Totarol in 0.1 M NaCl (pH 5.5) at a SR of 80 mV/s. RE: Hg/Hg_2Cl_2, KCl_{sat}

Figure 10 illustrates the increase in peak current over time, spanning from 0 to 4 minutes, before the sensor's surface becomes saturated and the peak current intensity decreases [35]. We consider 4 minutes to be the ideal accumulation time for the identification of the Totarol.

3.3.4. Concentration effect

Figure 11(A) displays the SWV voltammograms at varying Totarol concentrations, illustrating an increase in current intensity as the concentration increases. The corresponding calibration plot (Fig. 11B) exhibits a good linearity over 2 to 11.4 mM, with R^2 = 0.989, confirming the reliability of the sensor over this dynamic range. The resulting calibration equation is expressed as: I= 0.008 [C] + 1.264.

The detection limit (LOD = 3Sb/S) and the quantification limit (LOQ = 10Sb/S) were calculated, where Sb represents the standard deviation of five blank assessments and S is the slope of the calibration curve [36,37]. The corresponding results are summarized in Table 1.

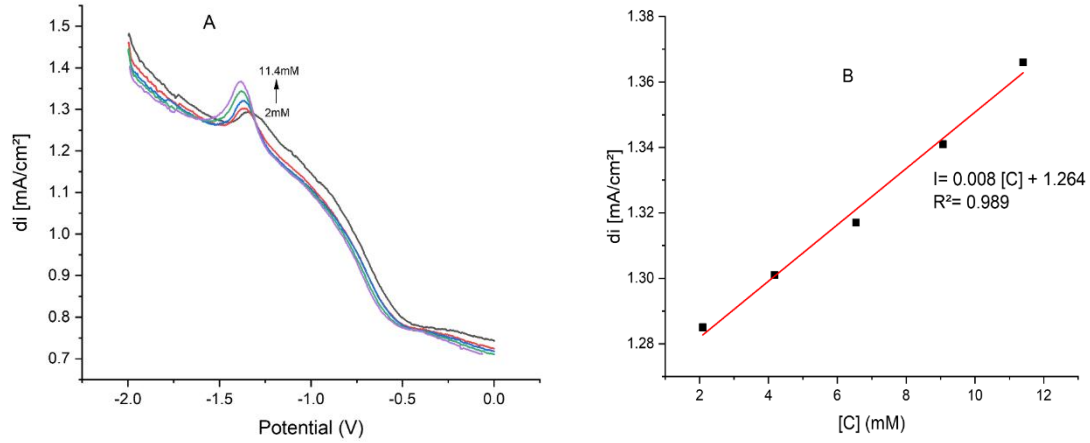

Figure 11. (A) SWV voltammograms of the sensor for the identification of the Totarol in 0.1 M NaCl pH= 5.5; amplitude: 20 mV; RE: Hg/Hg_2Cl_2, KCl_{sat} (B) Calibration graph of the Totarol

Table 1. LOQ and LOD values for the Totarol

Concentration range	LOQ	LOD
2-11.4 mM	3.94 µM	1.18 µM

3.3.5. Identification of the Totarol on the Tetraclinis articulata

For the quantitative determination of Totarol in the plant extract, 1 g of sample was first solubilized in 25 mL of 0.1 M NaCl in order to ensure adequate dispersion of the analyte. The study was executed by SWV within a potential window ranging from −2.0 V to 0.0 V. As

illustrated in Fig. 12, a well-defined anodic peak with a current intensity of 1.265 mA was observed at approximately −1.4 V, which is assigned to the response of Totarol, confirming its presence in the investigated extract. The concentration of Totarol was subsequently calculated using the previously established calibration curve, yielding a value of 0.125 mM/g of extract. This result provides a quantitative estimation of the Totarol content and allows for an evaluation of the extraction yield under the employed experimental conditions.

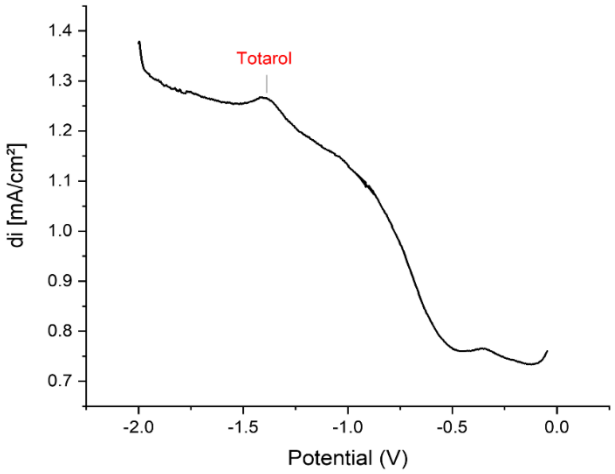

Figure 12. SWV voltammograms of the sensor for the identification of the Totarol in 1 g of the extract. Amplitude: 20 mV; RE: Hg/Hg_2Cl_2, KCl_{sat}

3.3.6. Reproducibility and stability studies

To assess the reproducibility of the sensor in the detection of totarol, multiple parallel measurements were investigated. As depicted in Figure 13, the findings demonstrated high consistency across electrodes prepared under identical conditions, confirming the method's excellent repeatability.

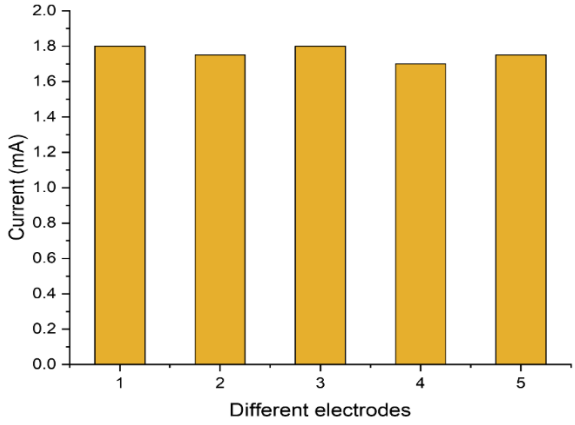

Figure 13. Reproducibility of the sensor with 2 mM of Totarol in 0.1 M NaCl (pH 4.5) at a SR of 80 mV/s. RE: Hg/Hg_2Cl_2, KCl_{sat}

Furthermore, the stability of the electrode was examined by measuring its response to a 2 mM totarol solution after two months of storage at room temperature. As illustrated in Fig. 14, the sensor preserved 98% of its starting current response, showing outstanding stability and reliability over time.

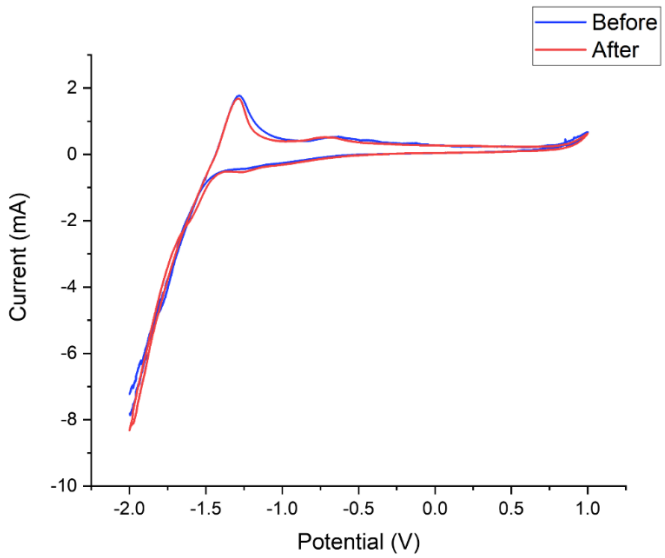

Figure 14. The stability of sensor with 2 mM of Totarol in a 0.1 M NaCl (pH 4.5) at a SR of 80 mV/s. RE: Hg/Hg_2Cl_2, KCl_{sat}

4. CONCLUSION

In summary, ZnO and $MgFe_2O_4$ NPs were efficiently synthesized and thoroughly characterized by FT-IR, SEM-EDX and XRD analysis. The nanomaterials were incorporated as modifier into a CPE to develop a sensitive sensor for the identification of Totarol. The performance of the ZnO–$MgFe_2O_4$/CPE was assessed using CV, EIS, and SWV. The developed sensor exhibited excellent electroanalytical characteristics, including enhanced electrocatalytic activity, a wide linear dynamic range, a low LOD, and satisfactory accuracy in the quantification of Totarol in Tetraclinis articulata extract. The obtained results highlight the potential of the proposed sensor as a reliable and practical tool for the monitoring of bioactive phenolic compounds in natural extracts and plant-derived pharmaceutical formulations.

List of abbreviations

CPE: Carbone past electrode
CV: Cyclic voltammetry
FR: Frequency range
FT-IR: Fourier-transform infrared
LOD: Detection limit
LOQ: Quantification limit
NPs: Nanoparticles
SEM: scanning electron microscopy
SR: Scan rate

SWV: Square wave voltammetry
TA: Tetraclinis articulata

Declarations of interest

The authors declare no conflict of interest in this reported work.

REFERENCES

[1] A. Ayed, L. Caputo, V. De Feo, F. Nazzaro, F. Fratianni, I. Amri, L. Hamrouni, Y. Mabrouk, and F. Polito, Chem. Biodivers. 22 (2024) e202401618.
[2] S. Khatib, O. Nerya, R. Musa, M. Shmuel, and S. Tamir, Bioorg. Med. Chem. 13 (2005) 433.
[3] W. Rached, F.Z. Zeghada, M. Bennaceur, L. Barros, R.C. Calhelha, S. Heleno, M. J. Alves, A. M. Carvalho, and A. Marouf, Ind. Crops Prod. 112 (2018) 460.
[4] M. Saber, H. Harhar, L. El Hattabi, G. Zengin, A. Bouyahya, and M. Tabyaoui, Int. J. Second. Metab. 8 (2021) 352.
[5] Y. Laamari, A. Oubella, A. Bimoussa, A. El Mansouri, E. M. Ketatni, O. Mentre, M. Y. Ait Itto, H. Morjani, M. Khouili, and A. Auhmani, Bioorg. Chem. 115 (2021) 105165.
[6] Y. Gao, X. Xu, S. Chang, Y. Wang, Y. Xu, S. Ran, Z. Huang, P. Li, J. Li, L. Zhang, J. M. Saavedra, H. Liao, and T. Pang, Toxicol. Appl. Pharmacol. 289 (2015) 142.
[7] S.I. Cuevas-Cianca, A.C.L. Leal, L.R. Hernández, E.S. Arreola, and H. Bach, Phytomed. Plus 2 (2022) 100357.
[8] G.E. Hyeon, and Y.B. Eom, Can. J. Microbiol. 70 (2024) 426.
[9] C. Shi, M. Che, X. Zhang, Z. Liu, R. Meng, X. Bu, H. Ye, and N. Guo, J. Food Sci. Technol. 55 (2018) 924.
[10] Z. Xu, S. Krajewski, T. Weindl, R. Loeffler, P. Li, X. Han, J. Geis-Gerstorfer, H. Wendel, L. Scheideler, and F. Rupp, Mater. Sci. Eng. C 110 (2020) 110701.
[11] S. Hoisang, S. Jitpean, S. Seesupa, P. Kamlangchai, T. Makpunpol, P. Ngowwatana, S. Chaimongkol, D. Khunbutsri, J. Khlongkhlaeo, and N. Kampa, Vet. Sci. 11 (2024) 437.
[12] H. Abo El-Kassem Bosly, J. King Saud Univ. Sci. 35 (2022) 102396.
[13] Y. Hou, X. Zhang, C. Wang, and M. Guo, Processes 8 (2020) 496.
[14] J. Kaal, J. Linderholm, and A. Martínez Cortizas, Anal. Pyrolysis Lett. 85 (2019) 408.
[15] A. Afkhami, F. Kafrashi, and T. Madrakian, Ionics 21 (2015) 1.
[16] L. Luo, D. Li, J. Zang, C. Chen, J. Zhu, H. Qiao, Y. Cai, K. Lu, X. Zhang, and Q. Wei, Energy Technol. 5 (2017) 1364.
[17] S. Raut, P. V. Thorat, and R. Thakre, Int. J. Sci. Res. 4 (2015) 1225.
[18] S. Kerouad, I. Forsal, A. Talfana, M. Kasbaji, and M. A. Edaala, Inorg. Chem. Commun. 177 (2025) 114232.

[19] T. Madrakian, H. Ghasemi, E. Haghshenas, and A. Afkhami, RSC Adv. 6 (2016) 33851.
[20] L. Moujir, A. Seca, A. Silva, and M. Barreto, Planta Med. 74 (2008) 751.
[21] C. Chikere, N. H. Faisal, P. K. T. Lin, and C. Fernandez, J. Phys.: Conf. Ser. 1310 (2019) 012008.
[22] K.R.S. Murthy, G.K. Raghu, and P. Binnal, J. Biotechnol. Bioeng. 5 (2021) 25.
[23] N. Kumar, G. Irfan, Udayabhanu, and G. Nagaraju, Mater. Today Proc. 8 (2021) 3116.
[24] K. Dulta, G. Koşarsoy Ağçeli, P. Chauhan, R. Jasrotia, and P.K. Chauhan, J. Clust. Sci. 33 (2022) 603.
[25] H. Hameed, A. Waheed, M. S. Sharif, M. Saleem, A. Afreen, M. Tariq, A. Kamal, W. A. Al-Onazi, D. A. Al Farraj, S. Ahmad, and R. M. Mahmoud, Micromachines 14 (2023) 928.
[26] X.T. Tran, T.T.L. Bien, T. V. Tran, and T.T.T. Nguyen, Nanoscale Adv. 6 (2024) 4885.
[27] O. Anor, S. Kerouad, F. Issam, W. Kotmani, M. Bouzaid, and L. Bouissane, RSC Sustainability 3 (2025) 4825.
[28] S. Kerouad, M.A. Edaala, I. Forsal, M. Ellaite, M. Kasbaji, M. Mbarki, and M. El Achaby, Nanoscale 17 (2025) 23139.
[29] N. Belarbi, F. Dergal, A.I. El-Haci, T. Attar, D. Lerari, B. Dahmani, C. Ait Ramdane-Terbouche, and K. Bachari, Anal. Bioanal. Electrochem. 13 (2021) 340.
[30] C. Laghlimi, Y. Ziat, A. Moutcine, M. Hammi, Z. Zarhri, O. Ifguis, and A. Chtaini, Chem. Data Collect. 31 (2021) 100496.
[31] Y. Beyene, Z. Bitew, and F. Fekade, Mater. Adv. 3 (2022) 5882.
[32] G. Tesfaye, N. Negash, and M. Tessema, BMC Chem. 16 (2022) 69.
[33] T. Imtiaz, A. Shah, N. Ullah, F.J. Iftikhar, I. Shah, S.M. Shah, and S.S. Shah, Water 5 (2022) 69.
[34] W.P. Wicaksono, H. Dang, S. Lee, and J. Choo, Appl. Surf. Sci. 649 (2024) 159163.
[35] C. Laghlimi, A. Moutcine, A. Chtaini, J. Isaad, A. Soufi, Y. Ziat, H. Amhamdi, and H. Belkhanchi, ADMET DMPK 11 (2023) 151.
[36] E.B. Kim, M. Imran, E.H. Lee, M. Shaheer Akhtar, and S. Ameen, Chemosphere 286 (2022) 131695.
[37] G. Li, S. Feng, L. Yan, L. Yang, B. Huo, L. Wang, and D. Yang, Food Chem. 404 (2023) 134609.